Cancer Pathogenesis and Therapy 1 (2023) 87–97

Contents lists available at ScienceDirect

Cancer Pathogenesis and Therapy

journal homepage: www.journals.elsevier.com/cancer-pathogenesis-and-therapy

Research article

miR-338-3p acts as a tumor suppressor in lung squamous cell carcinoma by targeting *FGFR2/FRS2*

Xia Shan [a,1], Cheng Zhang [b,1], Chunyu Li [c,1], Xingchen Fan [d], Guoxin Song [e], Jingfeng Zhu [f], Risheng Cao [g,***], Xiuwei Zhang [a,**], Wei Zhu [d,*]

[a] Department of Respiration, Jiangsu Province Hospital, And Nanjing Medical University First Affiliated Hospital, Nanjing, Jiangsu 210000, China
[b] Women & Children Central Laboratory, Jiangsu Province Hospital, And Nanjing Medical University First Affiliated Hospital, Nanjing, Jiangsu 210036, China
[c] Women & Children Intensive Care Unit, Jiangsu Province Hospital, And Nanjing Medical University First Affiliated Hospital, Nanjing, Jiangsu 210036, China
[d] Department of Oncology, Jiangsu Province Hospital, And Nanjing Medical University First Affiliated Hospital, Nanjing, Jiangsu 210029, China
[e] Department of Pathology, Jiangsu Province Hospital, And Nanjing Medical University First Affiliated Hospital, Nanjing, Jiangsu 210029, China
[f] Department of Nephrology, Jiangsu Province Hospital, And Nanjing Medical University First Affiliated Hospital, Nanjing, Jiangsu 210029, China
[g] Department of Science and Technology, Jiangsu Province Hospital, And Nanjing Medical University First Affiliated Hospital, Nanjing, Jiangsu 210029, China

HIGHLIGHTS

- The Cancer Genome Atlas (TCGA) and TargetScan databases support the relationship between miR-338-3p and fibroblast growth factor receptor substrate 2 (*FGFR2*).
- There is low expression of miR-338-3p in lung squamous cell carcinoma (LUSC) tissues and cells.
- *FGFR2* and fibroblast growth factor receptor substrate 2 (*FRS2*) were negatively correlated with miR-338-3p expression in LUSC tissues and cells.
- miR-338-3p targets *FGFR2* and *FRS2* in H1703 cells.
- miR-338-3p can inhibit LUSC cell proliferation and migration.

GRAPHICAL ABSTRACT

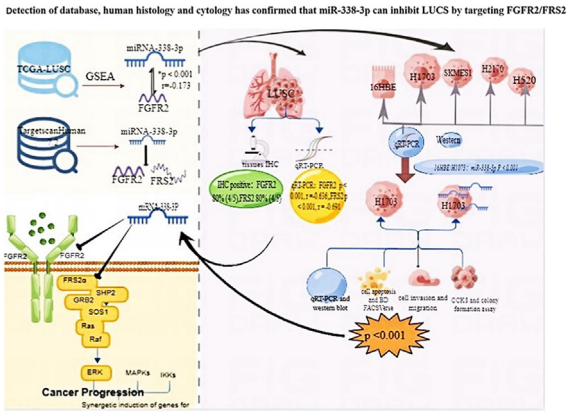

ARTICLE INFO

Managing Editor: Peng Lyu

Keywords:
miR-338-3p
FGFR2

ABSTRACT

Background: Lung cancer refers to the occurrence of malignant tumors in the lung, and squamous cell carcinoma is one of the most common pathological types of non-small cell lung cancer. Studies have shown that microRNAs (miRNAs) play an important role in the occurrence, development, early diagnosis, and treatment of lung cancer. This study aimed to explore the role and possible mechanism of MicroRNA-338-3p (miR-338-3p) in lung squamous cell carcinoma (LUSC).

* Corresponding author: Department of Oncology, the First Affiliated Hospital of Nanjing Medical University, 300 Guangzhou Road, Nanjing, Jiangsu 210029, China.
** Corresponding author: Department of Respiration, the Affiliated Jiangning Hospital of Nanjing Medical University, 169 Hushan Road, Nanjing, Jiangsu 210000, China.
*** Corresponding author: Department of Science and Technology, the First Affiliated Hospital of Nanjing Medical University, 300 Guangzhou Road, Nanjing, Jiangsu, 210029, China.
E-mail addresses: rishengcao@njmu.edu.cn (R. Cao), zhangxiuweiywy@126.com (X. Zhang), zhuwei@njmu.edu.cn (W. Zhu).
[1] Xia Shan, Cheng Zhang, and Chunyu Li are contributed equally to this study.

https://doi.org/10.1016/j.cpt.2022.12.004
Received 6 September 2022; Received in revised form 2 December 2022; Accepted 23 December 2022

FRS2
LUSC
Tumor suppressor

Method: In this study, we compared 238 LUSC patients with relatively high miR-338-3p expression levels with 238 miR-338-3p expression levels in The Cancer Genome Atlas (TCGA)-LUSC dataset using first-line gene set enrichment analysis (GSEA). Second, the mRNA expression of miR-338-3p, *FGFR2*, and fibroblast growth factor receptor substrate 2 (*FRS2)* in 30 lung cancers and adjacent lung tissues was detected using quantitative real-time polymerase chain reaction (qRT-PCR). Finally, *in vitro* experiments were conducted, whereby the expression levels of miR-338-3p in lung cancer cells (H1703, SKMES1, H2170, H520) and normal lung epithelial cells (16HBE) were detected using qRT-PCR. miR-338-3p was overexpressed in lung cancer cells (H1703), and the cell proliferation (cell counting kit-8 [CCK8] assay), colony formation, cell apoptosis, cell cycle (BD-FACSVerse assay, Becton Dickinson, Bedford, MA, USA), cell invasion, and migration (Transwell assay, Thermo Fischer Corporation, Waltham, MA, USA) were detected.
Results: We found that the expression of miR-338-3p was significantly reduced in LUSC tissues ($p < 0.001$) and cancer cell lines ($P < 0.01$), and miR-338-3p was significantly negatively correlated with the expression of *FGFR2* ($P < 0.001$) and *FRS2* ($P < 0.01$). Furthermore, overexpression of miR-338-3p inhibited proliferation ($P < 0.001$), migration, and invasion ($P < 0.001$) of LUSC cell lines and increased apoptosis in the G1 phase ($P < 0.001$) and cell cycle arrest ($P < 0.05$).
Conclusions: Our study demonstrates that miR-338-3p inhibits tumor cell proliferation and migration by targeting *FGFR2* and *FRS2* in LUSC. We believe that miR-338-3p may be a promising target for the treatment of LUSC.

Introduction

Lung cancer is the most common malignant tumor worldwide. In 2012, 1.8 million individuals were diagnosed with lung cancer, resulting in the death of 1.6 million individuals.[1] The American Cancer Society has estimated that approximately 236,740 new cases of lung cancer (117,910 in men and 118,830 in women) will be reported in the United States during 2022. Non-small cell lung cancer (NSCLC) accounts for approximately 80–85% of all lung cancer cases and can be divided into four histopathological subtypes as follows: lung adenocarcinoma (LUAD), lung squamous cell carcinoma (LUSC), large cell carcinoma, and neuroendocrine cancer. Studies have found that LUSC is a major type of NSCLC.[2–4] At present, most patients are found to be at an advanced stage of the disease at the time of their first diagnosis, with most patients also exhibiting poor treatment response and prognosis.[5–7] Approximately 30% of NSCLC patients are prone to distal metastasis after traditional molecular-targeted therapy or chemoradiotherapy, and the 5-year survival rate is less than 20%.[8–10] Unlike LUSC, the clinical outcomes of patients with LUAD have markedly improved due to the development of targeted therapies.[11–14] Therefore, to improve the treatment and prognosis of LUSC patients, further investigation of novel and effective therapeutic targets for LUSC is required.

MicroRNAs (miRNAs) are a class of small noncoding RNAs and are typically 18–25 nucleotides in length. It has been proven that miRNAs can modulate the expression of approximately one-third of human genes by binding to the 3′-untranslated region (UTR) of target messenger RNAs (mRNAs).[15] Several studies have demonstrated that miRNAs mediate a wide range of biological processes, including cell proliferation, cell cycle, apoptosis, and differentiation.[16–19] Moreover, aberrantly expressed miRNAs can disrupt systematically regulated RNA networks in several cancer types, including LUSC. MicroRNA-338-3p (miR-338-3p) is located on chromosome 17q25 and plays an important role in many cancers, such as prostate cancer, lymphoblastic lymphoma, ovarian cancer, renal carcinoma, and gastric cancer.[23] It has been reported that miR-372-3p promotes cell growth and metastasis by targeting *FGF9* in LUSC.[20] Furthermore, miR-375 is significantly downregulated in LUSC tissues and exerts a strong tumor-suppressive effect by targeting *PAX6*, *FOXG1*, and *WNT5A*.[21] Moreover, low expression of miR-448 has been found to be associated with poor prognosis in LUSC patients.[22] Although these findings provide novel insights into the molecular mechanisms underlying LUSC pathogenesis, the biological functions and molecular mechanisms of miR-338-3p in LUSC remain poorly understood.

In the present study, the expression levels of miR-338-3p were detected in patients with LUSC. The functions and potential mechanisms of miR-338-3p in LUSC were further explored to elucidate its role in LUSC development.

Methods

Clinical samples

Thirty pairs of histologically confirmed LUSC tissues and adjacent non-tumor lung tissues were obtained from patients with LUSC who had undergone a pneumonectomy at the First Affiliated Hospital of Nanjing Medical University between April 2015 and December 2016. All patients included in our study were newly diagnosed without any prior intervention. Pathological diagnosis of each sample was confirmed by an experienced pathologist. The fresh tissues were stored at −80 °C for subsequent experiments. The clinical characteristics of the patients with LUSC were recorded and are listed in Table 1.

Cell culture

Four LUSC cell lines (H1703, SKMES1, H2170, H520) and the human normal bronchial epithelial cell line (16HBE) were purchased from the American Type Culture Collection (ATCC). All cell lines were cultured in Dulbecco's modified Eagle's medium (DMEM) (Gibco, USA) supplemented with 10% fetal bovine serum (FBS) (HyClone, USA) and 100 U/mL penicillin and streptomycin (Invitrogen, CA) in the presence of 5% CO_2 at 37 °C.

Table 1
Correlation between clinicopathological features and miR-338-3p expression in human lung squamous cell carcinoma tissues.

Variables	Number of cases	miR-338-3p expression		χ^2	*P* value
		Low	High		
Age (years)				0.009	0.395
<55	3	2 (66.67)	1 (33.33)		
≥55	27	21 (77.78)	6 (22.22)		
Gender				0.003	0.418
Men	28	22 (78.57)	6 (21.43)		
Women	2	1 (50.00)	1 (50.00)		
TNM stage				0.582	0.372
I–II	20	14 (70.00)	6 (30.00)		
III–IV	10	9 (90.00)	1 (10.00)		
Tumor size (cm)				0.001	0.999
<5	26	20 (76.92)	6 (23.08)		
≥5	4	3 (75.00)	1 (25.00)		
Lymph node metastasis				0.001	0.999
No	25	19 (76.00)	6 (24.00)		
Yes	5	4 (80.00)	1 (20.00)		
Bronchial invasion				0.638	0.128
No	22	16 (72.73)	6 (27.27)		
Yes	8	7 (87.50)	1 (12.50)		

Data are presented as *n* (%). TNM: Tumor-node-metastasis.

Cell transfection

The cells were seeded in 24-well plates. miR-338-3p and negative control mimics were purchased from RiboBio Corporation (Guangzhou, China). Once cells reached 60% confluency, approximately 20 mmol/L Opti-MEM transfection media (Invitrogen, Thermo Fischer Corporation, Waltham, MA, USA) and Lipofectamine™ 2000 reagent (Life Technologies, Carlsbad, CA, USA) were used to transfect the cells following the manufacturer's instructions. Transfection efficiency was determined using qRT-PCR 48 h after transfection.

Quantitative reverse transcription polymerase chain reaction

Total RNA was isolated from clinical tissue samples and cultured cells using a one-step extraction method with TRIzol reagent (Invitrogen, Thermo Fischer Corporation, Waltham, MA, USA). Next, miRNAs were amplified using the Bulge-LoopTM miRNA qRT-PCR Primer Set (RiboBio, Guangzhou, China) with specific primers for reverse transcription and SYBR Premix Ex TaqTM II (Takara, Dalian, China). The procedures were performed using a 7900HT qRT-PCR system (Applied Biosystems, Foster City, CA, USA) according to the manufacturer's instructions. Three replicates were performed for each sample. The relative expression was calculated using the $2^{-\Delta\Delta Ct}$ method. The expression of U6 was used as an endogenous control for normalization.

Cell proliferation and colony formation assays

The CCK8 (Cell Counting Kit-8 ，CCK8) (Dojindo, Kumamoto, Japan) assay was performed to assess the cell proliferation rate. Briefly, the cells were seeded in 96-well plates at 5×10^3 cells/well. At specific transfection time points (24 h, 36 h, 48 h, 60 h, and 72 h), the cells were incubated in 10% CCK8 solution in a culture medium at 37 °C until a visual color conversion occurred. Absorbance was measured at 450 nm using a microplate reader (Bio-Tek Instruments, USA). For the colony formation assays, transfected cells were seeded into 6-well plates (5×10^3 cells/well) and cultured in DMEM supplemented with 10% FBS for 10 days. The media were then removed, and colonies were washed twice with phosphate-buffered saline (PBS). Finally, cells were fixed with 4% formaldehyde and stained with 0.1% crystal violet solution (Sigma–Aldrich, St. Louis, MI, USA) for 15 min. The number of colonies that were visible to the naked eye was counted using an inverted microscope. The rate of colony formation was calculated as colonies/transferred cells.

Cell migration and invasion assays

To examine the migratory ability of the cells *in vitro*, a Transwell assay was performed according to the manufacturer's instructions. Briefly, 5×10^3 cells were plated in the upper chamber of Transwell plates with serum-free DMEM, while the DMEM medium containing 10% FBS was added to the lower compartment. After 48 h of transfection, the cells were fixed in 4% formaldehyde for 20 min and stained with a 0.1% crystal violet solution. The number of migrated cells was determined in five random fields using an inverted microscope. For the invasion assay, the membranes of the upper chambers were pre-coated with 100 L of Matrigel (1 mg/mL). This assay was performed similarly to the migration assay.

Cell cycle and apoptosis assays

Cell cycle and apoptosis assays were performed 48 h after transfection. For the cell cycle assay, 5×10^3 transfected cells were cultured in 6-well plates in triplicate for 48 h. Next, the cells were collected and fixed in 70% ice-cold ethanol overnight at 4 °C, followed by incubation in 20 ug/mL propidium iodide (PI) (Sigma, USA) and 10 U/mL RNaseA at room temperature for 30 min in dark conditions. The collected cells were detected by Fluorescence-activated cell sorting (FACS) flow cytometry (FACSCalibur; Becton Dickinson, Bedford, MA, USA). For the cell apoptosis assay, the cells were harvested and suspended 48 h after transfection. Approximately 5 μL Annexin V-APC and 10 μL 7-AAD were added to the cell suspension. Annexin V-APC–positive cells were considered apoptotic.

Dual-luciferase reporter assay

The 3′UTR of human *FGFR2* and *FRS2* cDNA containing the putative target site for miR-338-3p (sequence shown in Supplementary Files 1 and 2) was chemically synthesized and inserted at the XbaI site, which is immediately downstream of the luciferase gene. *FRS2* (Fibroblast growth factor receptor substrate 2, *FRS2*)is a adapter protein that links activated FGR and NGF receptors to downstream signaling pathways. It plays an important role in the activation of MAP kinases and in the phosphorylation of PIK3R1, the regulatory subunit of phosphatidylinositol 3-kinase, in response to ligand-mediated activation of FGFR1. Modulates signaling via SHC1 by competing for a common binding site on NTRK1.Approximately 24 h before transfection, the cells were plated in 24-well plates at 1.5×10^5 cells/well. Next, 200 ng of pGL3-*FGFR2*-3′-UTR or pGL3-*FRS2*-3′-UTR plus 80 ng pRL-TK (Promega, Madison, WI, USA) was transfected in combination with 50 nM of the miR-338-3p mimic or miRNA mimic control, respectively, using lipofectamine 2000 reagent (Life Technologies, Carlsbad, CA, USA) according to the manufacturer's instructions. Luciferase activity was measured 24 h after transfection using the Dual-Luciferase Reporter Assay System (Promega, Madison, WI, USA). Firefly luciferase activity was normalized to Renilla luciferase activity in each transfected well. Three independent experiments were performed in triplicate.

Western blot analysis

H1703 cells were seeded in 6-well plates (6×10^5 cells/well). Approximately 48 h after transfection with the miR-338-3p mimic or miRNA mimic control, cultured cells were collected and lysed in RIPA (radioimmunoprecipitation assay, RIPA) lysis buffer, and the protein concentration was determined using the bicinchoninic acid assay (BCA) reagent kit (Beyotime, Jiangsu, China) according to the manufacturer's instructions. RIPA's full name is radioimmunoprecipitation buffer, it is a lysis buffer used to lyse cells or tissues, and is commonly used in radioimmunoprecipitation analysis. The proteins in samples were separated using 10% SDS-PAGE (sodium dodecyl sulfate-polyacrylamide gel electrophoresis, SDS-PAGE) and subsequently transferred to a PVDF (polyvinylidene difluoride, PVDF) membrane. PVDF is a highly non-reactive thermoplastic fluoropolymer. It can be synthesized by the polymerization of 1,1-difluoroethylene, and is soluble in strong polar solvents such as dimethylacetamide. It has excellent properties such as anti-aging, chemical resistance, weather resistance, and ultraviolet radiation resistance. It can be used as engineering plastics, used to make sealing rings and corrosion-resistant equipment, capacitors, and also used as coatings, insulating materials and ion exchange membrane materials. After the membranes were blocked with 5% non-fat milk for 2 h at room temperature, they were incubated at 4 °C with primary antibodies against *FGFR2* (catalog #23328, Cell Signaling Technology), *FRS2* (catalog: sc-17841, Santa Cruz Biotechnology), and β-actin (catalog: ab8245, Abcam), respectively, overnight. Finally, the membranes were incubated with horseradish peroxidase (HRP)-conjugated goat anti-mouse immunoglobulin (Ig)G antibody. Brand signals were visualized using enhanced chemiluminescence. The expression level of each protein was normalized to that of actin and the amount of protein loaded was calculated. The intensity of the protein bands was quantified using ImageJ software (National Institutes of Health, Bethesda, MD, USA).

Immunohistochemistry staining and scoring

Immunohistochemical staining was used to detect the expression of *FGFR2* and *FRS2* in five cases of lung cancer. Lung cancer tissue and adjacent normal tissue from all five cases were fixed, dehydrated, embedded, cut into 3–5 μm sections, Sections were then sequentially deparaffinized to water, antigen retrieved, and serum blocking. Next, the tissues were incubated with the primary rabbit monoclonal antibody against *FGFR2* and *FRS2* (1:100 dilution; *FGFR2*, #23328, Cell Signaling Technology; *FRS2*, sc-17841, Santa Cruz Biotechnology) for 12 h–15 h at 4 °C. After the tissue slides were washed, they were incubated with anti-rabbit secondary antibody for 1 h. The slides were then colored with 3,3-diaminobenzidine (DAB) (carrier laboratory), reverse stained with hematoxylin (carrier laboratory), dehydrated, treated with xylene, and sealed. All slides were examined, and representative images were taken using an Olympus BX41 microscope (Olympus America, Melville, NY).

Public database analyses

We analyzed the dataset of the TCGA-LUSC project for external validation. High-throughput transcriptome data and clinical phenotype information of 503 LUSC samples and 50 normal samples were downloaded using the Genomic Data Commons (GDC)-client tool. Raw count values for mRNA and miRNA mature strand expression were normalized using the "EdgeR" package (Bioconductor). Paired and unpaired Student's *t*-tests were used to compare gene expression levels between tumor tissues and normal controls. Pearson's correlation analysis was used to evaluate the relationship between miRNA and mRNA expression. Gene set enrichment analysis (GSEA) was performed to explore the potential pathways in which target miRNAs were highly involved.

Statistical analysis

Statistical analyses were performed using SPSS Version 25.0 (Armonk, NY), and diagrams were plotted using GraphPad Prism software, version 8.0 (GraphPad Software, San Diego, CA). The significance of any two groups was evaluated using a Student's *t*-test. The expression levels of miR-338-3p were compared between patients with varied clinical characteristics using the χ^2 test. The correlation between miRNA and mRNA expression was analyzed using Spearman's correlation analysis. A two-tailed $P < 0.05$ was regarded to be statistically significant ($P < 0.05$; $P < 0.01$; $P < 0.001$).

Results

miR-338-3p was significantly downregulated in lung squamous cell carcinoma tissues and cancer cell lines

Analysis of TCGA-LUSC data revealed that the expression level of miR-338 was significantly downregulated in LUSC tumor-like samples compared with that in normal tissue samples ($P < 0.001$) [Figure 1A and B]. We detected the expression of miR-338-3p in 30 LUSC tissues and adjacent non-tumor lung tissues using qRT-PCR. The results indicated that miR-338-3p expression was significantly lower in lung cancer tissues than that in paracancerous tissues ($P < 0.001$) [Figure 1C]. In addition, we examined the expression of miR-338-3p in lung cancer cells (H1703, SKMES1, H2170, H520) and human bronchial epithelial cells (16HBE). The results demonstrated that miR-338-3p expression was significantly decreased in all LUSC cell lines ($P < 0.01$) [Figure 1D]. The relationship between the basic clinical parameters of the patients and the expression level of miR-338-3p in LUSC tissues was analyzed. In 30 LUSC patients, the miR-338-3p expression levels were lower in LUSC tissues than in non-tumor lung tissues, suggesting a potential correlation between lower miR-338-3p expression and higher malignancy in LUSC ($P < 0.01$). Our results indicated that miR-338-3p was not significantly associated with factors such as age, tumor size, lymph node metastasis, or bronchial invasion, apart from sex ($P > 0.05$) [Table 1]. Furthermore, we found that miR-338-3p overexpression inhibited LUSC proliferation and induced apoptosis and cell cycle arrest.

GSEA was performed to compare 238 LUSC patients with relatively high expression levels of miR-338-3p (count value of miR-338-3p > 18,500) and 238 patients with low expression levels of miR-338-3p (count value of miR-338-3p < 14,400) in the TCGA-LUSC dataset. As shown in Supplementary File 3, lower miR-338-3p expression levels in LUSC patients were significantly associated with proliferation-relatedpathways, such as cell cycle DNA replication, DNA replication initiation, and sister chromatid condensation, whereas higher miR-338-3p expression indicated positive regulation of some immune-related pathways, including myeloid leukocyte migration, mast cell activation, and chemokine production.

To investigate the potential function of miR-338-3p in regulating LUSC cell proliferation and apoptosis, we transfected a miR-338-3p mimic into H1703 cells to establish miR-338-3p-overexpressed cells. The results of qRT-PCR demonstrated that the expression level of miR-338-3p in H1703 cells was significantly upregulated after transfection with the miR-338-3p mimic [Figure 2A]. A CCK8 assay was performed to test the effects of miR-338-3p on cell proliferation. The results indicated that overexpression of miR-338-3p significantly inhibited cell proliferation of H1703 cells between 48 h and 72 h after transfection [Figure 2B]. To analyze the cell cycle and cell apoptosis, a miR-338-3p mimic or negative control was transfected into H1703 cells and then detected using BD-FACSVerse. We found that the percentage of cells in the G1 phase significantly increased, while the percentage of cells in the S phase significantly decreased in H1703 cells transfected with miR-338-3p mimics when compared to the negative control [Figure 2C]. Furthermore, in the cell apoptosis assay, miR-338-3p overexpression significantly induced apoptosis [Figure 2D].

miR-338-3p overexpression inhibits LUSC cell metastasis

To gain further insight into the role of miR-338-3p in LUSC metastasis, colony formation, migration, and invasion assays were performed in H1703 cells transfected with a miR-338-3p mimic or negative control. We found that miR-338-3p overexpression significantly inhibited LUSC colony formation [Figure 3A], cell migration [Figure 3B], and cell invasion compared with the negative control group [Figure 3C].

FGFR2 and FRS2 were upregulated and negatively correlated with mir-338-3p in lung squamous cell carcinoma tissues

According to the search results of TargetscanHuman 7.2 (Bioinformatics and Research Computing [Whitehead Institute], Cambridge, MA), which is a curated database of mammalian miRNA targets (http://www.targetscan.org), *FGFR2* and *FRS2* are closely related to the tumorigenesis and progression of various tumors. These results indicate that *FGFR2* and *FRS2* are closely related to LUSC and are the direct targets of miR-338-3p in various species.

In our experiment, immunohistochemistry (IHC) and qRT-PCR were used to study the relationship between miR-338-3p, *FGFR2*, and *FRS2* in lung cancer tissues. First, we selected 30 pairs of tumor tissues and their adjacent lung tissues that were pathologically diagnosed as LUSC and used qRT-PCR to detect the mRNA expression of miR-338-3p, *FGFR2*, and *FRS2*. The results indicated that the mRNA expression levels of *FGFR2* and *FRS2* were significantly increased in LUSC tissues ($P < 0.001$; $P < 0.01$) [Figure 4A]. In addition, using Pearson's correlation analysis, we found that miR-338-3p was significantly negatively correlated with the expression levels of *FGFR2* and *FRS2* in LUSC tissues ($P < 0.001$, $r = -0.636$; $P < 0.001$, $r = -0.691$) [Figure 4B and C]. At the same time, we used five other pairs of LUSC tissues and their adjacent paracancerous lung tissues to detect protein expression using IHC. The results demonstrated that the positive rates of *FGFR2* and *FRS2* in LUSC tissues were 80% (4/5) and 80% (4/5), respectively.

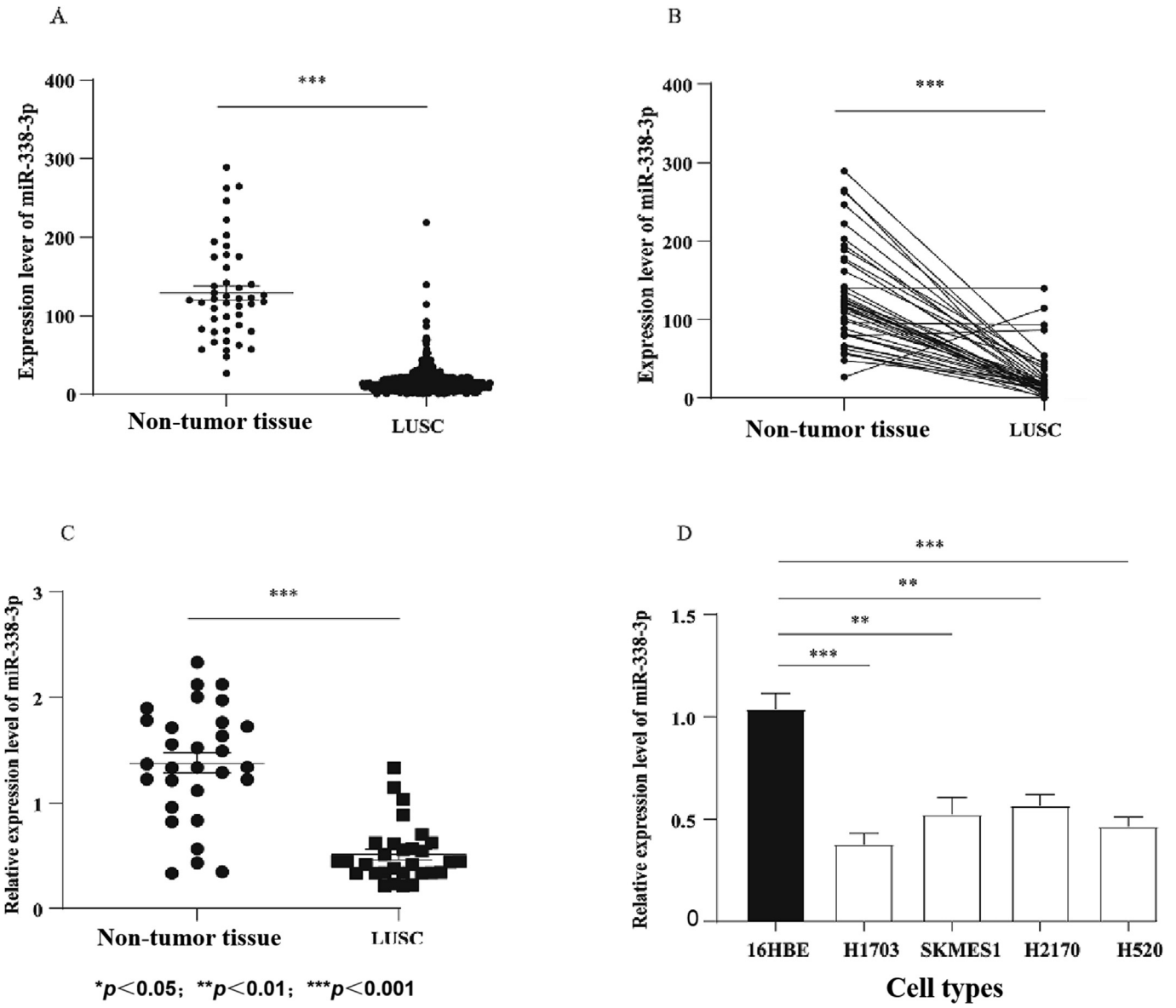

Figure 1. Expression of miR-338-3p in lung squamous cell carcinoma tissues and cell lines. miR-338-3p was significantly downregulated in LUSC tissues and four human LUSC cell lines. (A–B): Relative expression levels of miR-338-3p in human LUSC tissues and non-tumor lung tissues in the TCGA-LUSC dataset ($P < 0.001$) ([A] Student's *t*-test. [B] paired *t*-test). (C) The expression level of miR-338-3p in human LUSC tissues and adjacent normal tissues of 30 LUSC patients detected using qRT-PCR was significantly decreased ($P < 0.001$). (D) miR-338-3p expression levels were significantly reduced in four human LUSC cell lines (H1703, SKMES1, H2170, and H520) and a normal bronchial epithelial cell line (16HBE) ($P < 0.01$). LUSC: Lung squamous cell carcinoma; TCGA: The Cancer Genome Atlas.

FGFR2 was mainly expressed in the cytoplasm and membranes of LUSCs [Figure 4D and E], while *FRS2* was mainly expressed on the cell membranes of LUSCs [Figure 4F and G].

We also downloaded the RNA-Seq data of the TCGA-LUSC dataset and analyzed and compared the expression levels of *FGFR2* and *FRS2* in tumor and paracancerous lung tissues. The results indicated that the expression level of *FGFR2* was significantly upregulated in LUSC tissues ($P < 0.001$); however, the expression level of *FRS2* was not significantly increased in LUSC tissues ($p > 0.05$) [Supplementary Files A and B]. At the same time, we analyzed and compared tumor tissues and adjacent lung tissues and found that the expression levels of *FGFR2* and miR-338-3p were significantly negatively correlated ($P < 0.001$, $r = 0.173$), but the expression levels of *FRS2* and miR-338-3p were not significantly correlated ($p = 0.084$, $r = 0.079$) [Supplementary Files 4C and 4D]. IHC images in the Human Protein Atlas database (http://www.proteinatlas.org/) also demonstrated higher expression levels of *FGFR2* in LUSC tissues, whereas information on *FRS2* was missing. Overall, we found that miR-338-3p plays significant biological roles in LUSC by targeting *FGFR2* and *FRS2*.

The results obtained from searching TargetscanHuman 7.2 indicated that both *FGFR2* and *FRS2* are candidate targets of miR-338-3p. They are based on the target sequence at 103–109 bp of *FGFR2* 3′UTR and 266–272 bp of *FRS2* 3′UTR [Figure 5A]. Based on the above results, we used vectors containing the 3′-UTR of *FGFR2* or *FRS2* and fluorescent target sites of miR-338-3p downstream of the ribase gene (pGL3-*FGFR2*-3′-UTR and pGL3-*FRS2*-3′-UTR). H1703 cells were transfected with a luciferase reporter vector and a miR-338-3p mimic or miRNA mimic control. We found that relative luciferase activity was significantly reduced when pGL3-*FGFR2*-3′-UTR and pGL3-*FRS2*-3′-UTR were transfected with the miR-338-3p mimic compared to the miRNA mimic. These results confirmed that both *FGFR2* and *FRS2* are target genes of miR-338-3p ($P < 0.001$) [Figure 5B].

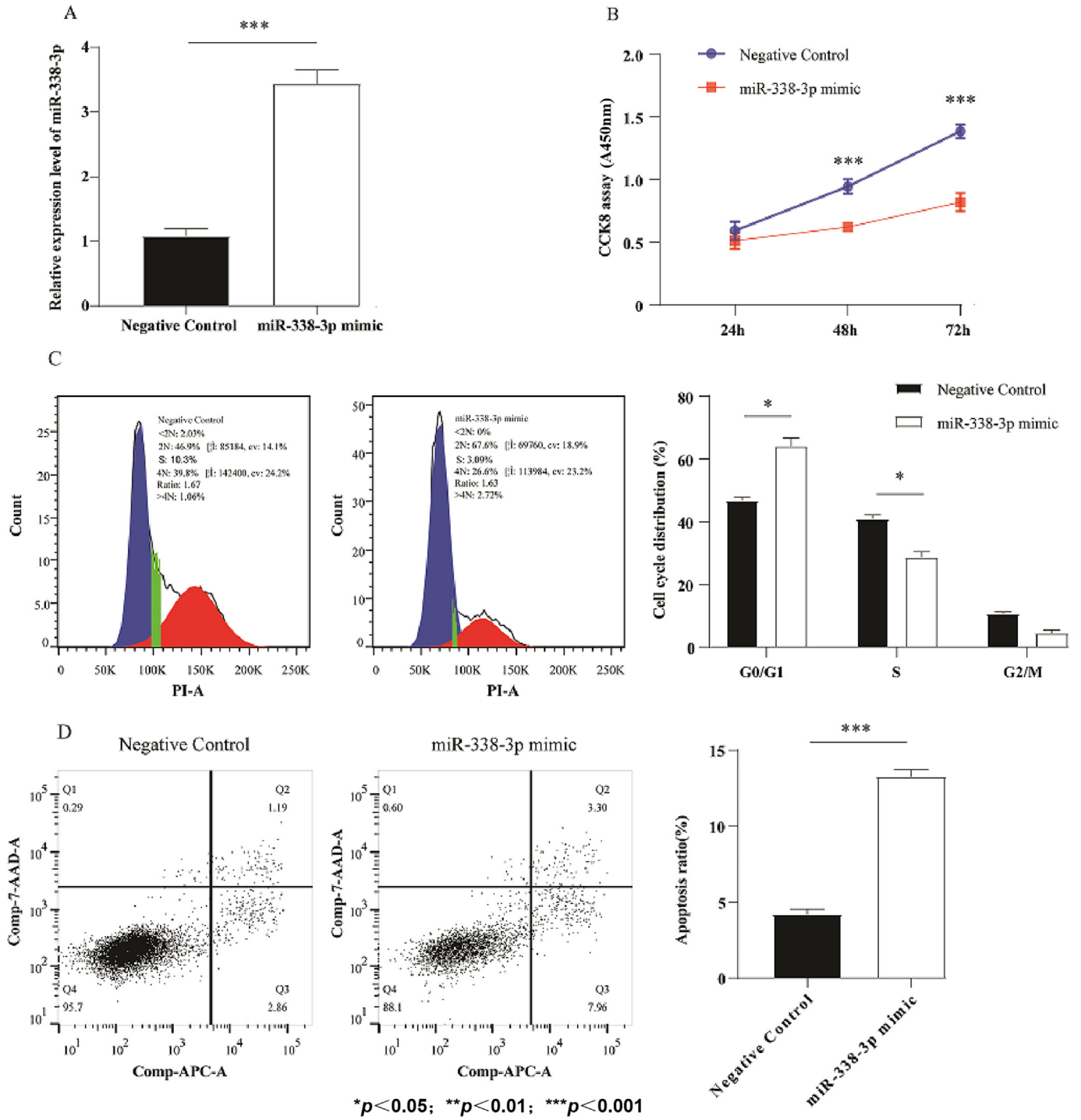

Figure 2. Effects of overexpressed miR-338-3p on cell proliferation, apoptosis, and cycle in LUSC H1703 cells. Overexpression of miR-338-3p in LUSC cells inhibited proliferation, apoptosis, and cell cycle. (A) The transfection efficiency of the miR-338-3p mimic or miRNA mimic control (negative control) was analyzed by qRT-PCR ($P < 0.001$). (B) Significant inhibition of cell proliferation was detected after transfection with miR-338-3p mimic or miRNA mimic control (negative control) ($P < 0.001$). (C) G0/G1 and S phase of the cell cycle were significantly prolonged ($P < 0.05$). (D) Cell apoptosis was significantly enhanced ($P < 0.001$). LUSC: Lung squamous cell carcinoma; qRT-PCR: Quantitative real-time polymerase chain reaction.

In the cell experiment, we performed qRT-PCR and Western blot analysis 48 h after the H1703 cells were transfected with miR-338-3p. The results indicated that the mRNA and protein levels of *FGFR2* and *FRS2* were significantly downregulated after transfection with the miR-338-3p mimic ($P < 0.001$) [Figure 5C and D]. These results suggest that miR-338-3p acts as a tumor suppressor in LUSC by targeting *FGFR2* and *FRS2*.

Discussion

Lung cancer poses a growing health burden worldwide.[24] LUSC is one of the major subtypes of NSCLC. Despite the high incidence of LUSC, there are no effective treatments for it. In recent years, targeted drug therapy, such as the currently used fibroblast growth factor receptor (FGFR)-targeted drugs, has gradually become the cornerstone of LUSC

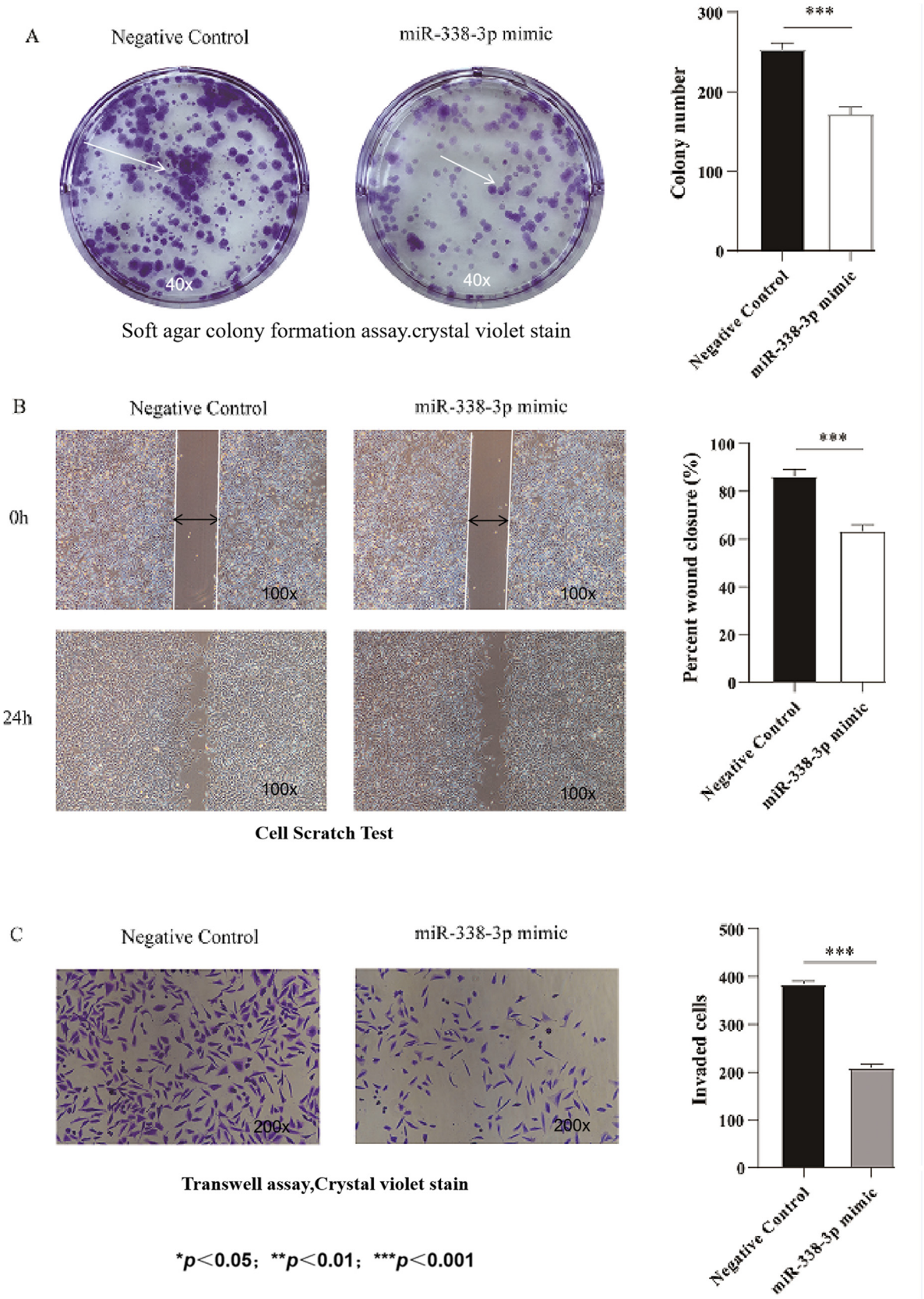

Figure 3. Overexpression of miR-338-3p inhibits the proliferation and migration of LUSC H1703 cells. Overexpression of miR-338-3p inhibited the proliferation and migration of LUSC H1703 cells. (A) The colonies in the colony formation test were significantly reduced ($P < 0.001$). (B) A cell scratch test was performed to explore the significantly reduced migration of LUSC cells ($P < 0.001$). (C) A Transwell test was performed, and we found that cell invasion was significantly weakened ($P < 0.001$). LUSC: Lung squamous cell carcinoma.

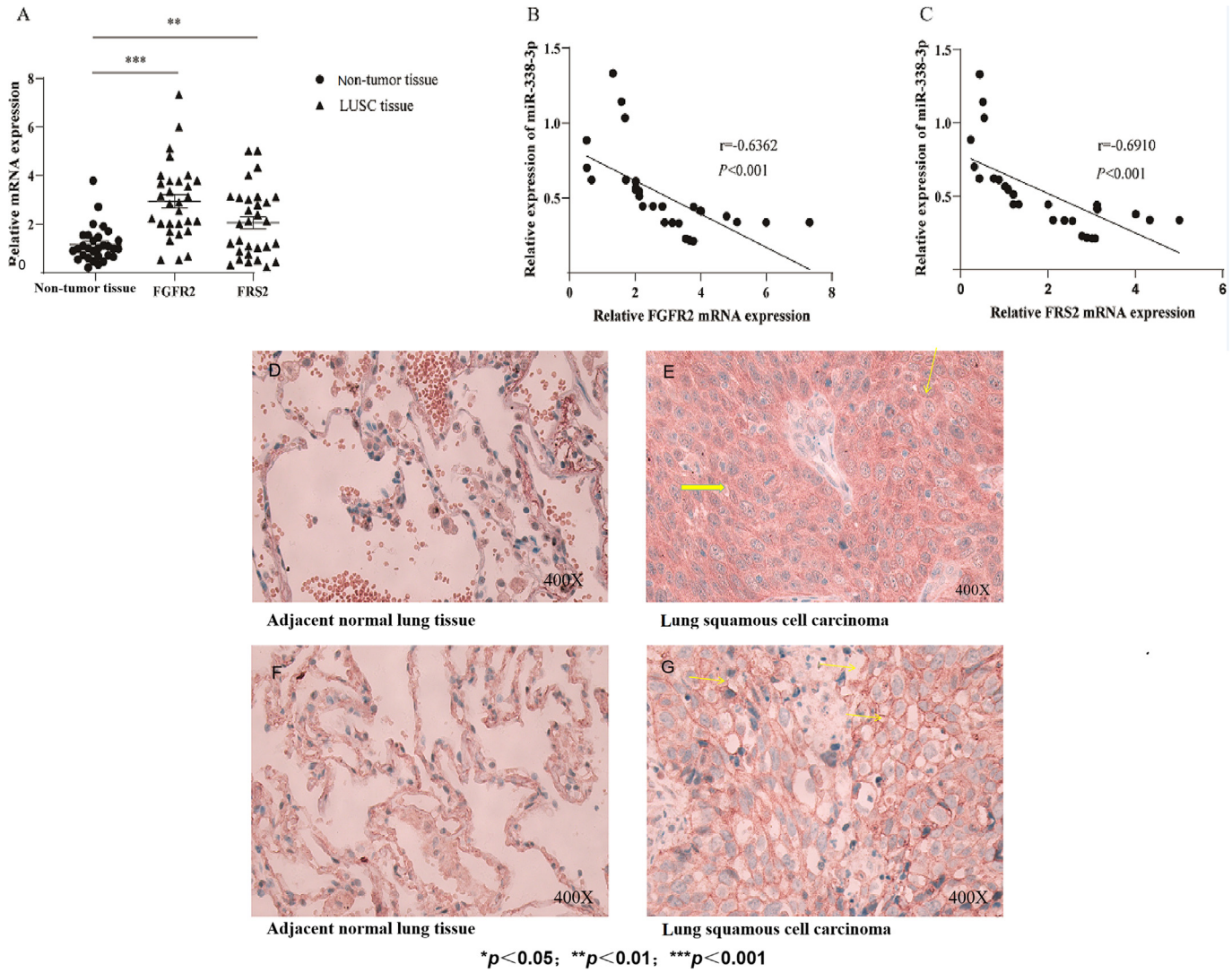

Figure 4. mRNA expression levels of *FGFR2* and *FRS2* in LUSC tissues and non-tumor lung tissues and their correlation with miR-338-3p. (A) Comparison of *FGFR2* and *FRS2* mRNA expression levels between LUSC tissues and non-tumor lung tissues. (B) Pearson correlation analysis of the expression levels of miR-338-3p and FGFR2 in LUSC tissues ($P < 0.001$, $r = -0.636$). (C) The correlation between the expression levels of miR-338-3p and FRS2 in LUSC tissues was analyzed using the Pearson correlation analysis ($P < 0.001$, $r = -0.691$). (D) The expression of FGFR2 in adjacent normal lung tissue (IHC 100 ×). (E) Expression of FGFR2 in LUSC tissues (IHC 400 ×). (F) The expression of FRS2 in adjacent normal lung tissue (IHC 100 ×). (G) FRS2 expression in LUSC tissues (IHC 400 ×). IHC: Immunohistochemistry; LUSC: Lung squamous cell carcinoma.

treatment. However, the clinical efficacy of FGFR-targeted drugs in LUSC patients is unsatisfactory, and only a small number of LUSC patients are able to obtain lasting benefits. Therefore, it is highly necessary to explore the underlying mechanisms that promote the development of LUSC and provide new directions for the treatment of LUSC in the future.

At present, miRNAs are known to bind to the 3′-UTR regions of target genes to inhibit gene expression and may exert critical biological functions.[25] miRNA-338-3p, which is located on chromosome 17q25, is downregulated and acts as a tumor suppressor in several cancer types, such as gastric cancer, prostate cancer, lymphoblastic lymphoma, and ovarian cancer[26–28]; however, its function in LUSC remains unknown. In this study, we observed a significant downregulation of miR-338-3p expression in LUSC tissues compared to that in normal tissues. In patients with substantial malignant clinicopathological features, such as larger tumor size, positive lymph node metastasis, and bronchial invasion, the expression levels of miR-338-3p were further reduced in tumor tissues. *In vitro* experiments demonstrated that overexpression of miR-338-3p significantly inhibited cell proliferation, induced apoptosis, and cell cycle arrest, and further inhibited cell migration and invasion in LUSC cells. These findings revealed that miR-338-3p could similarly act as a tumor suppressor for LUSC, which has rarely been reported before, and that the FGFR signaling pathway plays an important role in tumor growth and is a potential therapeutic target for a variety of tumors, especially LUSC.[29]

The *FGFR* family consists of four members, *FGFR1–FGFR4*, which are encoded by different genes. *FGFRs* are receptor tyrosine kinases that contain an extracellular ligand-binding site, transmembrane domain, and intracellular catalytic domain of activated kinases. Abnormal gene amplification and mutation of *FGFRs* are common in LUSC.[30] When the fibroblast growth factor (FGF) binds to *FGFRs*, receptor dimerization is induced, leading to transphosphorylation of the intracellular tyrosine kinase domain and activation of downstream signaling pathways.[31]

FGFR2, which is the cell surface receptor of the fibroblast growth factor, is a tyrosine-protein kinase that plays an important role in the regulation of cell proliferation, differentiation, migration, and apoptosis, as well as in the regulation of embryonic development. *FRS2* is an adapter protein that links activated FGR and NGF (Nerve growth factor, NGF) receptors to downstream signaling pathways. It plays an important role in the activation of MAP (mitogen-activated protein, MAP) kinases and in the phosphorylation of *PIK3R1*, which is the

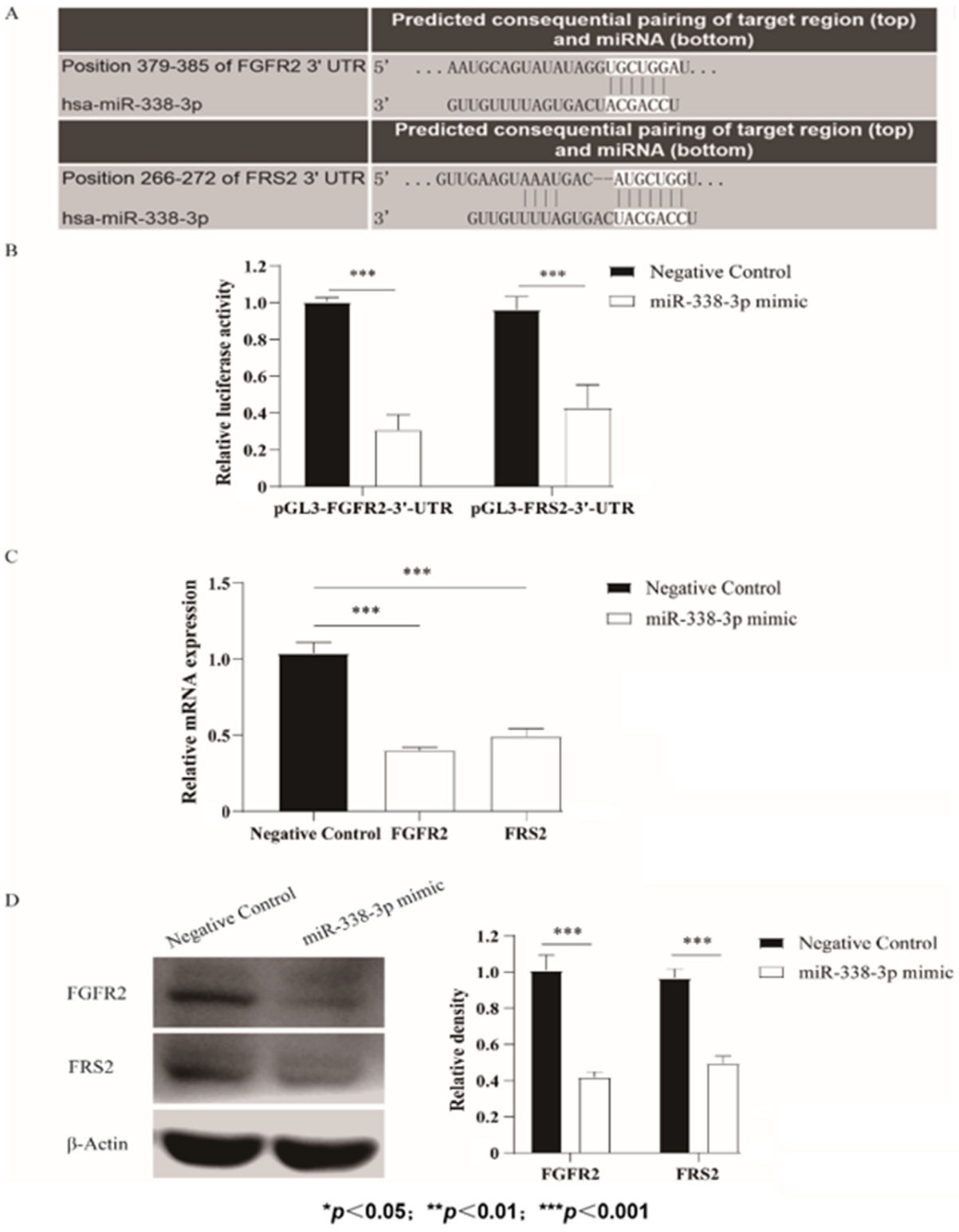

Figure 5. *FGFR2* and *FRS2* are direct target genes of miR-338-3p. (A) Predicted mRNA target regions and corresponding pairings of miR-338-3p. (B) Displays the relative fluorescence in H1703 cells when pGL3-FGFR2-3′-UTR or pGL3-FRS2-3′-UTR was transfected with the miR-338-3p mimic compared to the miRNA mimic control (negative control). Sulfatase activity decreased significantly ($P < 0.001$). (C) Compared with the miRNA mimic control (negative control), the mRNA expression levels of FGFR2 and FRS2 in H1703 cells were significantly downregulated after transfection with miR-338-3p mimic for 48 h ($P < 0.001$). (D) Approximately 48 h after transfection with the miR-338-3p mimic and miRNA mimic control, the protein expression levels of FGFR2 and FRS2 in H1703 cells were detected using Western blot ($P < 0.001$).

regulatory subunit of phosphatidylinositol 3-kinase, in response to ligand-mediated activation of *FGFR*. FGR is a member of the Src family of PTKs (protein tyrosine kinases, PTKs). The encoded protein contains N-terminal sites for myristylation and palmitylation, a PTK domain, and SH2 and SH3 domains which are involved in mediating protein–protein interactions with phosphotyrosine-containing and proline-rich motifs, respectively. Multiple alternatively spliced variants, encoding the same protein, have been identified. This gene is a proto-oncogene. NGF is

important for the development and maintenance of the sympathetic and sensory nervous systems.MAP is a particularly important component in the cascade reaction in the RTK-Ras signaling pathway after being phosphorylated.

It is well known that upon ligand binding by *FGFR2*, phosphorylation of *FGFR* substrate 2 (*FRS2*) triggers the recruitment of *GRB2, GAB1, PIK3R1*, and *SOS1*, and mediates the activation of RAS, MAPK1/ERK2, MAPK3/ERK1, and MAP kinases. Activated signaling pathways, as well as the *AKT1* signaling pathway, play important roles in tumor promotion.[32,33] It has also been reported that *FGFR2* overexpression promotes *STAT1* activation.

Bioinformatics analysis of the TargetscanHuman 7.2 database demonstrated that the two target sequences of miR-338-3p targeting *FGFR2* and *FRS2* were located at 103–109 bp of the *FGFR2* 3′UTR and 266–272 bp of the *FRS2* 3′UTR. The results of this study indicated that both the mRNA and protein expression levels of *FGFR2* and *FRS2* were significantly upregulated in LUSC, and a dual-luciferase reporter assay verified a significant negative correlation between miR-338-3p, *FGFR2*, and *FRS2*. The above results demonstrated that miR-338-3p could repress the expression of *FGFR2* and *FRS2* in LUSC by binding to the 3′-UTR region of *FGFR2* and *FRS2* mRNA, respectively.

Study limitation

This study has some limitations. First, our findings are only applicable to the Chinese population and may not be applicable to other countries, and the sample size is small. Second, due to ethical reasons, there was a lack of control samples from healthy individuals.

In conclusion, the results of our study indicate that miR-338-3p is downregulated in both LUSC tissue and LUSC cells. Furthermore, *FGFR2* and *FRS2* are the target genes of miR-338-3p, and the biological functions of miR-338-3p may be implemented by targeting *FGFR2* and *FRS2* in LUSC cells. Importantly, miR-338-3p may inhibit lung cancer cell proliferation and migration, at least through the direct targeting of *FGFR2* and *FRS2*, thus activating RAS, MAPK1/ERK2, MAPK3/ERK1, and MAP kinase signaling pathways in H1703 cells. These data indicate that miR-338-3p may be a promising target for the treatment of LUSC.

Funding

None.

Author contributions

Xia Shan designed the study, collected and analyzed the data, and completed basic experiments. Cheng Zhang and Chunyu Li contributed to the experiments, writing, and performing the statistical analysis. Xingchen Fan, Guoxin Song, and Jingfeng Zhu contributed to writing the manuscript. Cao and Zhang conceived and coordinated the experiments and were responsible for the final substance. Wei Zhu is the guarantor and supervisor of this work and has full and ultimate responsibility for the methodology, completeness, and curation of data analysis. All authors revised and approved the final version of the manuscript for publication.

Ethics statement

This study was approved by the Medical Ethics Committee of the First Affiliated Hospital of Nanjing Medical University (Ethics Code:2016-SRFA-148), and written informed consent was obtained from all participants involved.

Data availability statement

The data that support the funding of this study are available on request from the corresponding author and are not publicly available due to privacy or ethical restrictions.

Conflict of interest

None.

Acknowledgment

This study was supported by Professor Li Hai and others from the Department of Pathology.

Appendix A. Supplementary data

Supplementary data to this article can be found online at https://doi.org/10.1016/j.cpt.2022.12.004.

References

1. National Lung Screening Trial Research Team. Lung cancer incidence and mortality with extended follow-up in the national lung screening trial. *J Thorac Oncol*. 2019;14:1732–1742. https://doi.org/10.1016/j.jtho.2019.05.044.
2. Brainard J, Farver C. The diagnosis of non-small cell lung cancer in the molecular era. *Mod Pathol*. 2019;32(1):16–26. https://doi.org/10.1038/s41379-018-0156-x.
3. Nagano T, Tachihara M, Nishimura Y. Molecular mechanisms and targeted therapies including immunotherapy for non-small cell lung cancer. *Curr Cancer Drug Targets*. 2019;19:595–630. https://doi.org/10.2174/1568009619666181210114559.
4. Wang Y, Zou S, Zhao Z, Liu P, Ke C, Xu S. New insights into small-cell lung cancer development and therapy. *Cell Biol Int*. 2020;44:1564–1576. https://doi.org/10.1002/cbin.11359.
5. Bade BC, Dela Cruz CS. Lung cancer 2020: epidemiology, etiology, and prevention. *Clin Chest Med*. 2020;41:1–24. https://doi.org/10.1016/j.ccm.2019.10.001.
6. Goebel C, Louden CL, McKenna Jr R, Onugha O, Wachtel A, Long T. Diagnosis of non-small cell lung cancer for early stage asymptomatic patients. *Cancer Genomics Proteomics*. 2019;16:229–244. https://doi.org/10.21873/cgp.20128.
7. Waqar SN, Morgensztern D. Treatment advances in small cell lung cancer (SCLC). *Pharmacol Ther*. 2017;180:16–23. https://doi.org/10.1016/j.pharmthera.2017.06.002.
8. Murakami S. Durvalumab for the treatment of non-small cell lung cancer. *Expert Rev Anticancer Ther*. 2019;19:1009–1016. https://doi.org/10.1080/14737140.2019.1699407.
9. Cheema PK, Rothenstein J, Melosky B, Brade A, Hirsh V. Perspectives on treatment advances for stage III locally advanced unresectable non-small-cell lung cancer. *Curr Oncol*. 2019;26:37–42. https://doi.org/10.3747/co.25.4096.
10. Robinson SD, Tahir BA, Absalom KAR, et al. Radical accelerated radiotherapy for non-small cell lung cancer (NSCLC): a 5-year retrospective review of two dose fractionation schedules. *Radiother Oncol*. 2020;143:37–43. https://doi.org/10.1016/j.radonc.2019.08.025.
11. Saab S, Zalzale H, Rahal Z, Khalifeh Y, Sinjab A, Kadara H. Insights into lung cancer immune-based biology, prevention, and treatment. *Front Immunol*. 2020;11:159. https://doi.org/10.3389/fimmu.2020.00159.
12. Duma N, Santana-Davila R, Molina JR. Non-small cell lung cancer: epidemiology, screening, diagnosis, and treatment. *Mayo Clin Proc*. 2019;94:1623–1640. https://doi.org/10.1016/j.mayocp.2019.01.013.
13. Hirsch FR, Scagliotti GV, Mulshine JL, et al. Lung cancer: current therapies and new targeted treatments. *Lancet*. 2017;389:299–311. https://doi.org/10.1016/S0140-6736(16)30958-8.
14. Herbst RS, Morgensztern D, Boshoff C. The biology and management of non-small cell lung cancer. *Nature*. 2018;553:446–454. https://doi.org/10.1038/nature25183.
15. Ali Syeda Z, Langden SSS, Munkhzul C, Lee M, Song SJ. Regulatory mechanism of microRNA expression in cancer. *Int J Mol Sci*. 2020 Mar 3;21:1723. https://doi.org/10.3390/ijms21051723.
16. Khan S, Ayub H, Khan T, Wahid F. MicroRNA biogenesis, gene silencing mechanisms and role in breast, ovarian and prostate cancer. *Biochimie*. 2019;167:12–24. https://doi.org/10.1016/j.biochi.2019.09.001.
17. Tomar D, Yadav AS, Kumar D, Bhadauriya G, Kundu GC. Non-coding RNAs as potential therapeutic targets in breast cancer. *Biochim Biophys Acta Gene Regul Mech*. 2020;1863, 194378. https://doi.org/10.1016/j.bbagrm.2019.04.005.
18. Si W, Shen J, Zheng H, Fan W. The role and mechanisms of action of microRNAs in cancer drug resistance. *Clin Epigenet*. 2019;11:25. https://doi.org/10.1186/s13148-018-0587-8.
19. Chen X, Xie D, Zhao Q, You ZH. MicroRNAs and complex diseases: from experimental results to computational models. *Briefings Bioinf*. 2019;20:515–539. https://doi.org/10.1093/bib/bbx130.
20. Wang Q, Liu S, Zhao X, Wang Y, Tian D, Jiang W. MiR-372-3p promotes cell growth and metastasis by targeting FGF9 in lung squamous cell carcinoma. *Cancer Med*. 2017;6:1323–1330. https://doi.org/10.1002/cam4.1026.
21. Chen WJ, Gan TQ, Qin H, et al. Implication of downregulation and prospective pathway signaling of microRNA-375 in lung squamous cell carcinoma. *Pathol Res Pract*. 2017;213:364–372. https://doi.org/10.1016/j.prp.2017.01.007.

22. Shan C, Fei F, Li F, et al. miR-448 is a novel prognostic factor of lung squamous cell carcinoma and regulates cells growth and metastasis by targeting DCLK1. *Biomed Pharmacother*. 2017;89:1227–1234. https://doi.org/10.1016/j.biopha.2017.02.017.
23. Wang Y, Qin H. miR-338-3p targets RAB23 and suppresses tumorigenicity of prostate cancer cells. *Am J Cancer Res*. 2018;8:2564–2574.
24. Siegel RL, Miller KD, Fuchs HE, Jemal A. Cancer statistics, 2021. *CA A Cancer J Clin*. 2021;71:7–33. https://doi.org/10.3322/caac.21654.
25. Patel SA, Weiss J. Advances in the treatment of non-small cell lung cancer: Immunotherapy. *Clin Chest Med*. 2020;41:237–247. https://doi.org/10.1016/j.ccm.2020.02.010.
26. Luan X, Wang Y. LncRNA XLOC_006390 facilitates cervical cancer tumorigenesis and metastasis as a ceRNA against miR-331-3p and miR-338-3p. *J Gynecol Oncol*. 2018;29:e95. https://doi.org/10.3802/jgo.2018.29.e95.
27. He J, Wang J, Li S, Li T, Chen K, Zhang S. Hypoxia-inhibited miR-338-3p suppresses breast cancer progression by directly targeting ZEB2. *Cancer Sci*. 2020;111:3550–3563. https://doi.org/10.1111/cas.14589.
28. Chu CA, Lee CT, Lee JC, et al. MiR-338-5p promotes metastasis of colorectal cancer by inhibition of phosphatidylinositol 3-kinase, catalytic subunit type 3-mediated autophagy pathway. *EBioMedicine*. 2019;43:270–281. https://doi.org/10.1016/j.ebiom.2019.04.010.
29. Wu M, Wang G, Tian W, Deng Y, Xu Y. MiRNA-based therapeutics for lung cancer. *Curr Pharmaceut Des*. 2018;23:5989–5996. https://doi.org/10.2174/1381612823666170714151715.
30. Khan AQ, Ahmed EI, Elareer NR, Junejo K, Steinhoff M, Uddin S. Role of miRNA-regulated cancer stem cells in the pathogenesis of human malignancies. *Cells*. 2019;8:840. https://doi.org/10.3390/cells8080840.
31. Luo Y, Yang C, Jin C, Xie R, Wang F, McKeehan WL. Novel phosphotyrosine targets of FGFR2IIIb signaling. *Cell Signal*. 2009;21:1370–1378. https://doi.org/10.1016/j.cellsig.2009.04.004.
32. Sévère N, Miraoui H, Marie PJ. The Casitas B lineage lymphoma (Cbl) mutant G306E enhances osteogenic differentiation in human mesenchymal stromal cells in part by decreased Cbl-mediated platelet-derived growth factor receptor alpha and fibroblast growth factor receptor 2 ubiquitination. *J Biol Chem*. 2011;286:24443–24450. https://doi.org/10.1074/jbc.M110.197525.
33. Persaud A, Alberts P, Hayes M, et al. Nedd4-1 binds and ubiquitylates activated FGFR1 to control its endocytosis and function. *EMBO J*. 2011;30:3259–3273. https://doi.org/10.1038/emboj.2011.234.